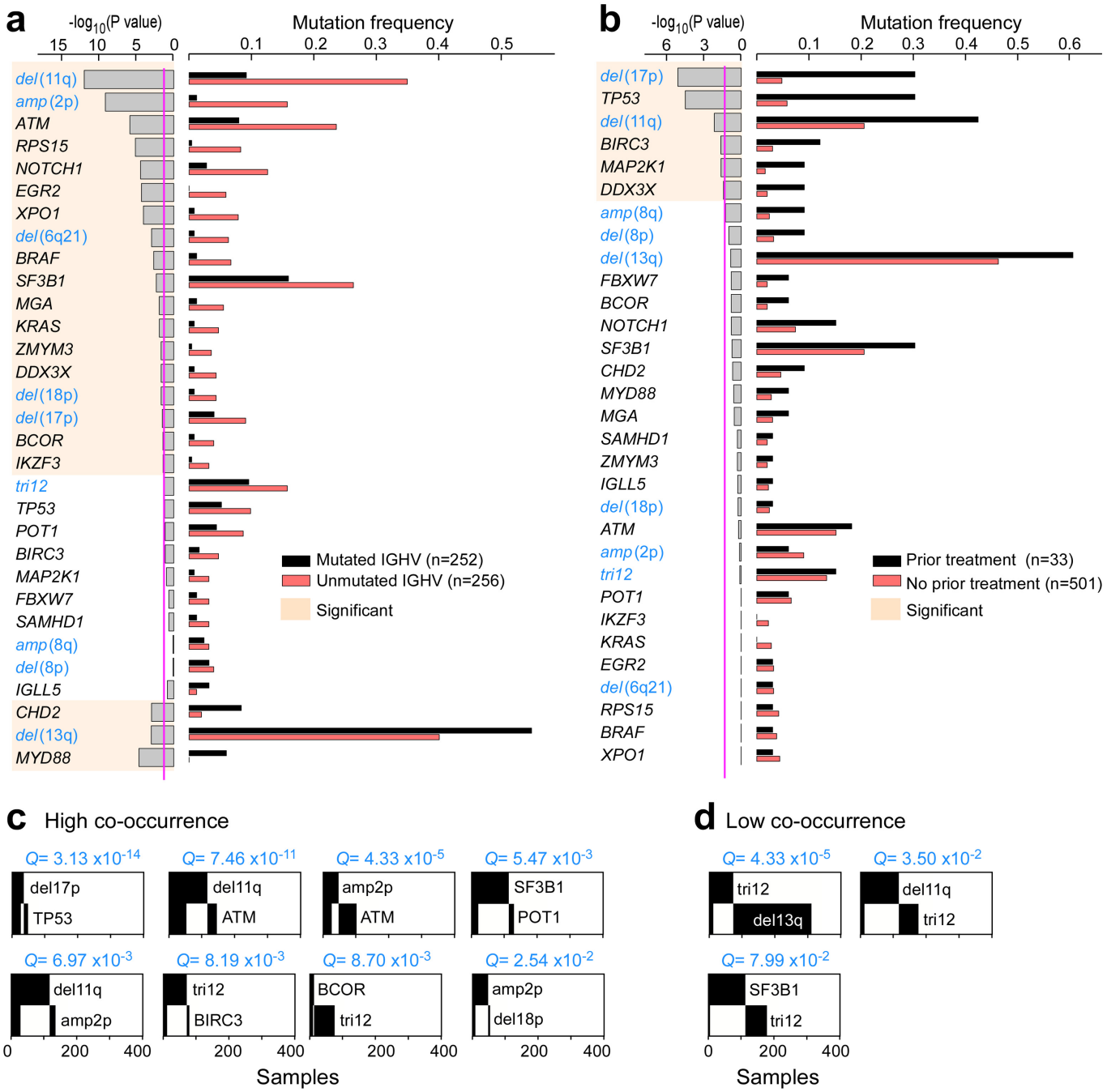

Extended Data Figure 6 | Annotation of drivers based on clinical characteristics and co-occurrence patterns. **a**, Putative drivers affecting greater than 10 patients were assessed for enrichment in *IGHV* mutated versus unmutated CLL subtype (Fisher's exact test, magenta line denotes $P = 0.05$). **b**, Putative drivers affecting greater than 10 patients were assessed for enrichment in samples that received therapy before sampling (Fisher's exact test). Putative drivers affecting greater than 10 patients were tested for co-occurrence. **c**, **d**, Significantly high (**c**) or low (**d**) co-occurrences are shown ($Q < 0.1$, Fisher's exact test with Benjamini Hochberg, false discovery rate, after accounting for prior therapy and *IGHV* mutation status, see Supplementary Methods).

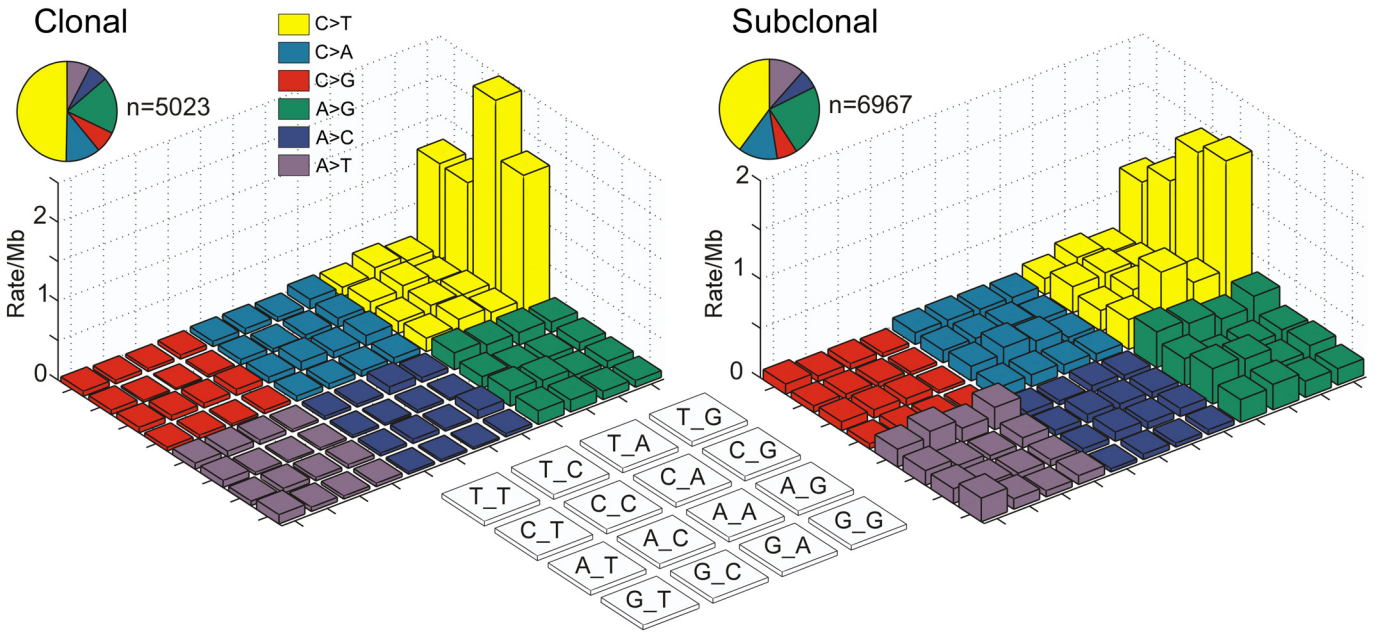

Extended Data Figure 7 | Mutation spectrum analysis, clonal versus subclonal sSNVs. The spectrum of mutation is shown for the clonal and subclonal subsets of coding somatic sSNVs across WES of 538 samples. The rate is calculated by dividing the number of trinucleotides with the specified sSNVs by the covered territory containing the specified trinucleotide. Both clonal and subclonal sSNVs were similarly dominated by C > T transitions at CpG sites. Thus, this mutational process that was previously associated with ageing[39] not only predates oncogenic transformation (since clonal mutations will be highly enriched in mutations that precede the malignant transformation[40]) but also is the dominant mechanism of malignant diversification after transformation in CLL.

39. Alexandrov, L. B. *et al.* Signatures of mutational processes in human cancer. *Nature* **500,** 415–421 (2013).
40. Vogelstein, B. *et al.* Cancer genome landscapes. *Science* **339,** 1546–1558 (2013).

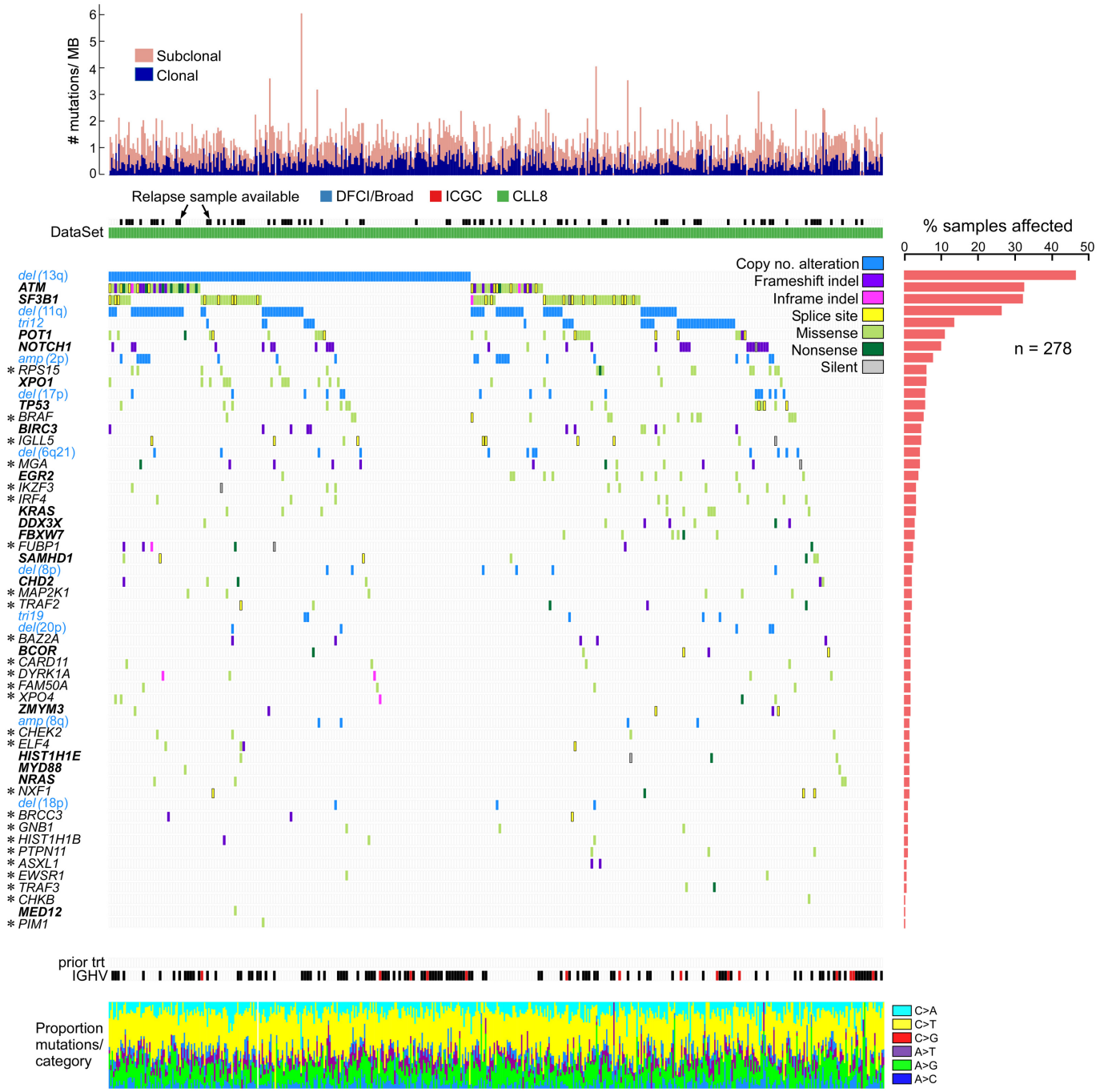

Extended Data Figure 8 | The CLL driver landscape in the CLL8 cohort. Somatic mutation information shown across the 55 candidate CLL cancer genes and recurrent somatic CNAs (rows) for 278 CLL samples collected from patients enrolled on the CLL8 clinical trial primary that underwent WES (columns). Recurrent somatic CNA labels are listed in blue, candidate CLL cancer genes are listed in bold if previously identified in Landau *et al.*[3], and with an asterisk if newly identified in the current study.

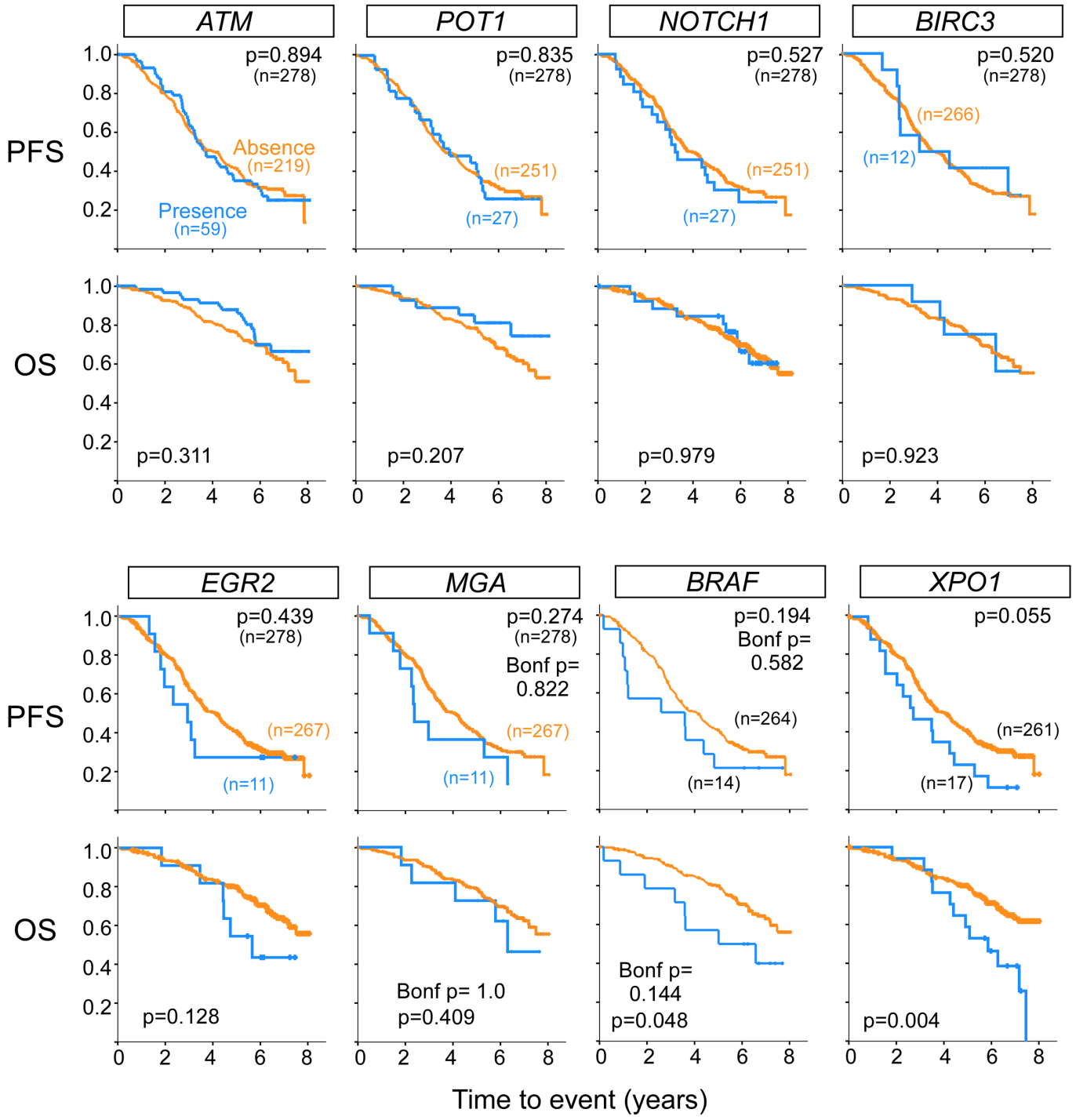

Extended Data Figure 9 | CLL8 patient cohort clinical outcome (from 278 patients) information by CLL cancer gene. Kaplan–Meier analysis (with logrank *P* values) for putative drivers not associated with significant impact on progression-free survival (PFS) or overall survival (OS) in the cohort of 278 patients that were treated as part of the CLL8 trial. For candidate CLL genes tested here for the first time regarding impact on outcome, a Bonferroni *P* value is also shown.

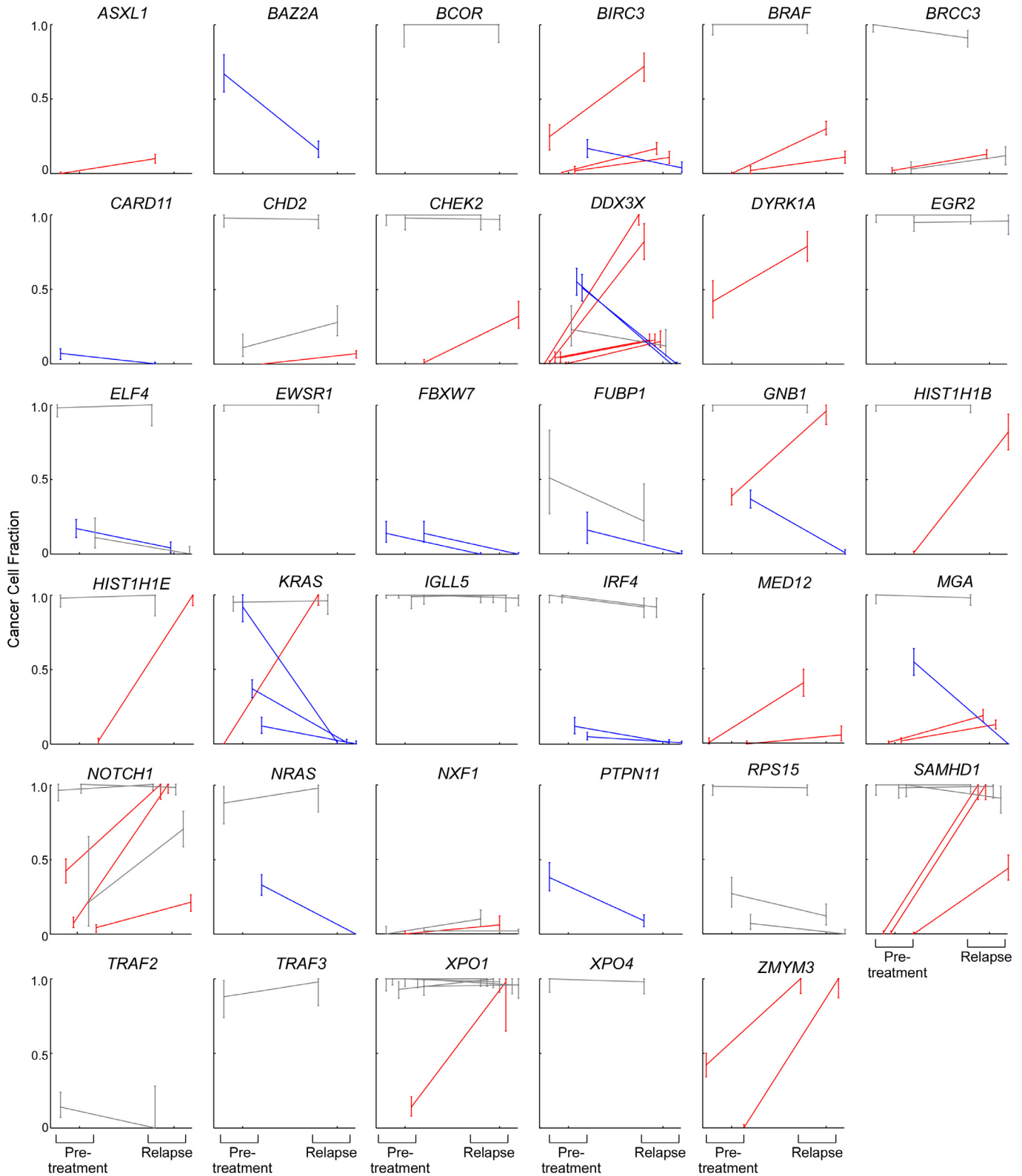

Extended Data Figure 10 | Comparison of pre-treatment and relapse cancer cell fraction (CCF) for non-silent mutations in candidate CLL genes across 59 CLLs. For each CLL gene mutated across the 59 CLLs that were sampled longitudinally, the modal CCF is compared between the pre-treatment and relapse samples. CCF increases (red), decreases (blue) or stable CCF (grey) over time are shown (in addition to CLL genes shown in Fig. 5). A significant change in CCF over time (red or blue) was determined if the 95% CI of the CCF in the pre-treatment and relapse samples did not overlap.